



Contents lists available at ScienceDirect

## International Dairy Journal

journal homepage: [www.elsevier.com/locate/idairyj](http://www.elsevier.com/locate/idairyj)

# Rapid detection of *Salmonella* in milk by biofunctionalised magnetic nanoparticle cluster sensor based on nuclear magnetic resonance



Dengchao Zou, Ling Jin, Bin Wu, Liwen Hu, Xingguang Chen, Ganhui Huang, Jinsheng Zhang\*

State Key Laboratory of Food Science and Technology, Nanchang University, Nanchang, 330047, PR China

## ARTICLE INFO

## Article history:

Received 19 August 2018

Received in revised form

9 November 2018

Accepted 10 November 2018

Available online 29 December 2018

## ABSTRACT

Controlling foodborne pathogens is important to ensure food safety and prevent foodborne diseases. In this study, a  $\text{Fe}_3\text{O}_4$  nanoparticle cluster ( $\text{Fe}_3\text{O}_4$  NPC) biosensor based on nuclear magnetic resonance was developed for *Salmonella* detection. The capture antibody of *Salmonella* was used, and the biotinylated antibody specifically recognised *Salmonella* at different sites.  $\text{Fe}_3\text{O}_4$  NPC modified with streptavidin were used to capture biotinylated antibody by biotin and determine streptavidin interaction. Finally,  $\text{Fe}_3\text{O}_4$  NPC immobilised on 96-well microplates were eluted, thereby reducing the transverse relaxation time ( $T_2$ ) of neighbouring water molecules. The method detected *Salmonella* at  $10^5$  cfu  $\text{mL}^{-1}$ , which was also the limit of detection in spiked milk samples, and showed high selectivity over other non-target bacteria. The proposed biosensor could be a potential tool for sensitive and rapid detection of foodborne pathogens in food, environmental, and agricultural samples.

© 2018 Elsevier Ltd. All rights reserved.

## 1. Introduction

Foodborne bacteria have caused extensive concern worldwide (Kant et al., 2018; Law, Ab Mutalib, Chan, & Lee, 2015). Milk and dairy products have become an essential part of the daily diet because of their abundant nutrients (Claeys et al., 2014), but can be contaminated by pathogenic bacteria. A report from the Centers for Disease Control and Prevention (Costard, Espejo, Groenendaal, & Zagmutt, 2017) indicated the occurrence of 81 outbreaks of food diseases associated with raw milk and raw milk cheese from 2007 to 2012. Among foodborne bacteria, *Salmonella* is considered a common pathogen in milk (Wang et al., 2016). Thus, a rapid and sensitive technology needs to be developed to help control the quality of milk.

Traditional methods for identification of foodborne pathogens are typically based on culture combined with standard biological tests; these methods require repetitive steps of enrichment and biological tests and would take 4–7 days to obtain a reliable result (D'Amico & Donnelly, 2009). To address the long processing time used in traditional methods, researchers have established rapid methods for detection of foodborne pathogens. These methods include polymerase chain reaction (PCR) (Bai et al., 2018; Zhou

et al., 2017), enzyme-linked immunosorbent assay (ELISA) (Galikowska et al., 2011; Jain et al., 2012), surface plasmon resonance (SPR) (Mazumdar, Barlen, Kampfer, & Keusgen, 2010; Son, Kim, Kothapalli, Morgan, & Ess, 2007). PCR exhibits high sensitivity, but requires cell disruption and nucleic acid extraction and precise and expensive instruments (Zhang et al., 2016). ELISA can detect a wide range of foodborne bacteria due to its specificity and sensitivity, but is labour intensive and time consuming (Wang et al., 2015). SPR biosensors do not require labels, but have limited application due to their poor sensitivity and high cost (Taylor et al., 2006). Therefore, a rapid, sensitive, and accurate method needs to be developed for *Salmonella* detection.

Magnetic nanoparticles conjugated with molecules that impart specificity, such as antibodies and oligonucleotides, possess inherent magnetic features and potential applications and have gained increasing attention in medical, environmental, and biochemical analyses (Gruskiene et al., 2018; Matthew, 2018; Zheng et al., 2013). Biological and environmental samples exhibit negligible magnetic background (Alcantara, Lopez, Garcia-Martin, & Pozo, 2016; Haun, Yoon, Lee, & Weissleder, 2010). The combination of magnetic nanoparticles and NMR could be used for analysis of turbid samples (Cai et al., 2011a; Shen et al., 2014). In recent years, NMR biosensors have been rapidly developed and widely applied to quantify and identify a wide range biological targets, including metal ions (Yang et al., 2016; Yang, Tian, Wang, & Yang, 2012; Zhang

\* Corresponding author. Tel.: +86 791 8396 9146.

E-mail address: [zhangjinsheng@ncu.edu.cn](mailto:zhangjinsheng@ncu.edu.cn) (J. Zhang).

et al., 2015), nucleic acids (Grimm, Perez, Josephson, & Weissleder, 2004), proteins (Cai et al., 2011b; Colombo et al., 2009; Kim, Josephson, Langer, & Cima, 2007), viruses (Perez, Simeone, Saeki, Josephson, & Weissleder, 2003), algal toxins (Ma et al., 2009), and bacteria (Chen et al., 2013; Wang et al., 2015; Zhao et al., 2017). However, these biosensors manifest a common phenomenon called the high-dose hook effect, in which the high concentrations of the analyte saturate the receptor and prevent the aggregation of nanoparticles (Kim et al., 2007). This phenomenon is a limitation of all agglutination assays and interferes with detection.

Herein, we conduct a novel NMR biosensor based on nuclear magnetic resonance for detection of *Salmonella* in milk (Fig. 1). In this assay,  $\text{Fe}_3\text{O}_4$  magnetic nanoparticles (NP) were used as probe. Signal amplification methods including streptavidin-biotin system and magnetic nanoparticle cluster were adopted to improve the sensitivity of the NMR biosensor. Compared with individual  $\text{Fe}_3\text{O}_4$  NP,  $\text{Fe}_3\text{O}_4$  NPC synthesised by individual  $\text{Fe}_3\text{O}_4$  NP conjugated with poly-L-lysine (PLL) exhibits the collective effect, which leads to a high reduction of transverse relaxation time ( $T_2$ ). To our knowledge, this study is the first to develop a NMR biosensor combined with  $\text{Fe}_3\text{O}_4$  NPC for detection of large molecular antigens.

## 2. Materials and methods

### 2.1. Chemicals and equipment

1-(3-Dimethylaminopropyl)-3-ethylcarbodiimide hydrochloride (EDC·HCl) and hydroxy-2,5-dioxypyridine-3-sulfonic acid sodium salt (NHSS) were obtained from Aladdin (Shanghai, China). Poly-L-lysine (PLL; 30–70 kDa) was provided by Sigma–Aldrich Chemical Co (St. Louis, MO, USA). Carboxylated magnetic nanoparticles with 180 nm diameter ( $10 \text{ mg mL}^{-1}$ ) were provided by

Allrunnano Technology Co. Ltd. (Shanghai, China). Streptavidin was purchased from Hualan Technology Co. (Shanghai, China). Anti-*Salmonella* capture antibody and detection antibody were supplied by Alpha–Lifetech (San Francisco, CA, USA). Long-chain biotin was obtained from Thermo Fisher Scientific Inc. (Rockford, IL, USA). Polystyrene microplates (96 wells) were obtained from Jet Biofil (Guangzhou, China). A 0.5 T EDUMR20-015V-I NMR was provided by Shanghai Niumag Electronic Technology Co. Ltd. (Shanghai, China). Pasteurised milk was obtained from a local grocery store.

### 2.2. Bacterial strains, culture media, and growth conditions

The following strains were obtained from the American Type Culture (ATCC), China Medical Culture Collection (CMCC), and Plant Variety Protection Act (PVPA): *Salmonella* (ATCC 9270), *Listeria monocytogenes* (ATCC 19115), *Proteus bacillus vulgaris* (CMCC 49027), *Pseudomonas aeruginosa* (CMCC 11997), and *Shigella sonnei* (Jiangxi CDC isolates). All strains were grown in brain heart infusion broth on a shaking incubator at 180 rpm and 37 °C overnight. PBS (0.01 M, pH 7.4) was used to dilute bacteria to obtain different concentrations of the cell suspension. Bacterial concentration was determined by counting the colonies grown on LB plates after incubation at 37 °C for 24 h.

### 2.3. Synthesis and characterisation of $\text{Fe}_3\text{O}_4$ NPC

$\text{Fe}_3\text{O}_4$  NPC were synthesised using previously reported methods (Liu et al., 2011; Zhang et al., 2016). In brief, 0.5 mg EDC·HCl was mixed with 1 mg  $\text{Fe}_3\text{O}_4$  NP in 1 mL PBS (0.01 M, pH 7.4) on a vertical mixer at room temperature for 30 min. The solution was then added with different amounts of PLL. The mixture was reacted for 4 h at 37 °C.  $\text{Fe}_3\text{O}_4$  NPC was obtained

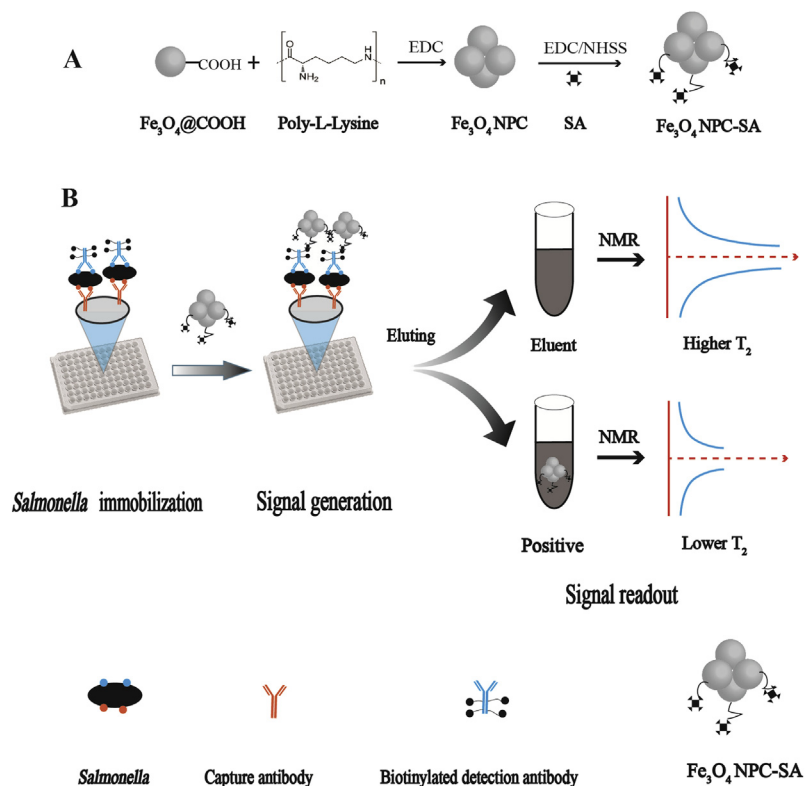


Fig. 1. NMR biosensor based on nuclear magnetic resonance for detection of *Salmonella*: (A) representation for preparation of  $\text{Fe}_3\text{O}_4$  NPC and  $\text{Fe}_3\text{O}_4$  NPC-SA; (B) overview of NMR biosensor for detection of *Salmonella* in milk.

after removing the excess EDC·HCl and PLL by using an external magnetic field. After washing three times, Fe<sub>3</sub>O<sub>4</sub> NPC were re-suspended in 1 mL PBS containing 0.2% NaN<sub>3</sub> and stored at 4 °C until use in experiment.

The hydrodynamic size and size distribution of Fe<sub>3</sub>O<sub>4</sub> NPC were measured by Zetasizer Nano ZS90 (Zeta Sizer Nano ZS90, Malvern Instruments Ltd., Britain). The scanning electron microscopy (SEM) images of Fe<sub>3</sub>O<sub>4</sub> NPC and Fe<sub>3</sub>O<sub>4</sub> NP were recorded (JSM-6701F, JEOL Ltd., Tokyo, Japan) (Meng, Li, Li, Xiong & Xu, 2004).

#### 2.4. Synthesis of Fe<sub>3</sub>O<sub>4</sub> NPC-SA and biotin-antibody

Fe<sub>3</sub>O<sub>4</sub> NPC-SA was synthesised by conjugating SA on Fe<sub>3</sub>O<sub>4</sub> NPC. In brief, 0.5 mg EDC·HCl and 0.5 mg NHSS were added to 1 mg Fe<sub>3</sub>O<sub>4</sub> NPC in PBS (0.01 M, pH 7.4) on the vertical mixer at 37 °C for 30 min. After washing with PBST (PBS with 0.05% Tween) for three times to remove unreacted EDC·HCl and NHSS, streptavidin (SA) (100 µg) was added to conjugate with Fe<sub>3</sub>O<sub>4</sub> NPC via amidation reaction. The mixture was reacted for 4 h at 37 °C, and the conjugate was washed three times with PBST (PBS with 0.05% Tween) and blocked with 1% (w/v) BSA solution for 45 min at 37 °C. Fe<sub>3</sub>O<sub>4</sub> NPC-SA was obtained after removing excess BSA by using an external magnetic field. After washing three times, the resulting Fe<sub>3</sub>O<sub>4</sub> NPC-SA was re-suspended in 1 mL of PBS containing 0.2% NaN<sub>3</sub> and stored at 4 °C until use in the experiment.

Biotin-antibody was prepared by mixing NHSS activated long-chain biotin and anti-*Salmonella* detection antibodies in PBS (0.01 M, pH 7.4) with molar ratios of 50:1 and incubated at room temperature for 45 min. Free long-chain biotin was removed by ultrafiltration centrifugation (filtration 30 kDa) at 6000×g for 6 min. Finally, glycerin was added to the as-prepared biotin-antibody solution to a final concentration of 50% and stored at -20 °C prior to use.

#### 2.5. NMR assay

The schematic of NMR biosensor is illustrated in Fig. 1. First, 96-well microplates were coated with the capture antibody (100 µL well<sup>-1</sup>) in PBS (0.01 M, pH 7.4) overnight at 4 °C. The plates were washed three times with PBST (300 µL well<sup>-1</sup>) to remove unbound antibody. Each well was blocked with 1% BSA (200 µL well<sup>-1</sup>) for 2 h at 37 °C. After repeating the washing, each well was injected with PBS (300 µL well<sup>-1</sup>) and stored until use.

After removing PBS in the microplates, 10-fold serial bacterial solution (100 µL well<sup>-1</sup>) was injected to the well for 1 h at 37 °C. The plate was washed three times, and biotin-antibody (100 µL well<sup>-1</sup>) was injected into the well for 1 h at 37 °C. The washing step was repeated, and the Fe<sub>3</sub>O<sub>4</sub> NPC-SA solution (100 µL well<sup>-1</sup>) was injected into the well for 1 h at 37 °C. The unbound Fe<sub>3</sub>O<sub>4</sub> NPC-SA was removed, and the plate was washed three times. The eluent (200 µL well<sup>-1</sup>) was injected into the well and incubated for 10 min at room temperature. Finally, the solution was collected and measured by NMR. The following equation was used to calculate  $\Delta T_2$ :

$$\Delta T_2 = T_{2\text{eluent}} - T_{2\text{sample}}$$

where  $T_{2\text{eluent}}$  is the average  $T_2$  of the eluent, and  $T_{2\text{sample}}$  is the average  $T_2$  of the eluent containing Fe<sub>3</sub>O<sub>4</sub> NPC after the addition of *Salmonella*.

#### 2.6. Evaluation of specificity and sensitivity of NMR biosensor

Four bacterial strains, namely, *Salmonella* (ATCC 9270), *L. monocytogenes* (ATCC 19115), *P. vulgaris* (CMCC 49027), and

*P. aeruginosa* (CMCC 11997), and *Shigella* (Jiangxi CDC isolates) were used to test the specificity of the NMR biosensor. The concentrations of these strains were 10<sup>7</sup> cfu mL<sup>-1</sup>. Additionally, 100 µL of PBS (0.01 M, pH 7.4) instead of the bacterial strain was used as negative control.

A series of concentrations of *Salmonella* (8.6 × 10<sup>1</sup>–8.6 × 10<sup>7</sup> cfu mL<sup>-1</sup>) was prepared to determine the limit of detection (LOD) of the NMR biosensor under the optimal conditions. Each sample was tested three times by NMR.

#### 2.7. Detection of *Salmonella* in spiked milk samples

Pasteurised milk was spiked with *Salmonella* at different concentrations and assayed by the proposed method. In brief, 10 mL of milk was added into 90 mL of PBS (0.01 M, pH 7.4) to form a 10% homogenate. The *Salmonella* solutions were spiked to the above homogenates with *Salmonella* final concentrations ranging from 8.6 × 10<sup>1</sup> cfu mL<sup>-1</sup> to 8.6 × 10<sup>7</sup> cfu mL<sup>-1</sup>. After coating the antibody overnight and blocking with 1% BSA for 2 h, the spiked milk samples (100 µL well<sup>-1</sup>) were injected into the well for 1 h at 37 °C. The remaining process was conducted as described previously. All samples were analysed by NMR. The experiment was performed in triplicate.

### 3. Results

#### 3.1. Characterisation of Fe<sub>3</sub>O<sub>4</sub> NPC

As shown in Fig. 2A, the hydrodynamic size and size distribution of Fe<sub>3</sub>O<sub>4</sub> NPC obtained with different Fe<sub>3</sub>O<sub>4</sub>/PLL ratios were determined using dynamic light scattering particle size analyser (Zeta Sizer Nano ZS90, Malvern Instruments Ltd, Worcestershire, UK). In comparison with Fe<sub>3</sub>O<sub>4</sub> NP, the mean hydrodynamic size of Fe<sub>3</sub>O<sub>4</sub> NPC increased gradually when the amount of PLL added was increased from 2 µg to 8 µg. The size distribution of Fe<sub>3</sub>O<sub>4</sub> NPC presented similar profiles, with the central peak position moving toward the large size shown in Fig. 2B. Most importantly, after reaction with PLL, Fe<sub>3</sub>O<sub>4</sub> NPC did not appear unwanted or formed huge agglomerates in the single-light scattering profiles. When the amount of PLL was further increased (10 µg), Fe<sub>3</sub>O<sub>4</sub> NPC became typical polydisperse nanoparticles with poor colloidal stability under ambient conditions. Therefore, 8 µg of PLL was selected as the optimal amount for synthesis of Fe<sub>3</sub>O<sub>4</sub> NPC.

To obtain further evidence with regard to the successful preparation of Fe<sub>3</sub>O<sub>4</sub> NPC, we performed SEM characterisation on Fe<sub>3</sub>O<sub>4</sub> NP and Fe<sub>3</sub>O<sub>4</sub> NPC. Fig. 2C shows that Fe<sub>3</sub>O<sub>4</sub> NP presented a dispersed state when the solution was sufficiently diluted. Meanwhile, Fe<sub>3</sub>O<sub>4</sub> NP had a tendency to form a close-packed structure when the concentration of Fe<sub>3</sub>O<sub>4</sub> NP was increased. However, Fe<sub>3</sub>O<sub>4</sub> NPC still presented aggregates of magnetic particles even after dilution, as shown in Fig. 2D.

#### 3.2. Characterisation of Fe<sub>3</sub>O<sub>4</sub> NPC-SA

After the conjugation with PLL, Fe<sub>3</sub>O<sub>4</sub> NPC still possessed carbonyl groups and could conjugate with streptavidin via amidation reaction. To obtain evidence that streptavidin was already conjugated with Fe<sub>3</sub>O<sub>4</sub> NPC, we performed DLS characterisation on Fe<sub>3</sub>O<sub>4</sub> NPC and Fe<sub>3</sub>O<sub>4</sub> NPC-SA. As shown in Fig. 3A, after conjugation with streptavidin, the average hydrodynamic size of Fe<sub>3</sub>O<sub>4</sub> NPC-SA was found to be 397.7 nm. In comparison with Fe<sub>3</sub>O<sub>4</sub> NPC, the hydrodynamic size of Fe<sub>3</sub>O<sub>4</sub> NPC-SA was increased by 118 nm. Taking 10 nm for the mean hydrodynamic size of IgG (150 kDa) (Jans, Liu, Austin, Maes, & Huo, 2009), the average hydrodynamic size of streptavidin (66 kDa) was found to be lower than that of IgG.

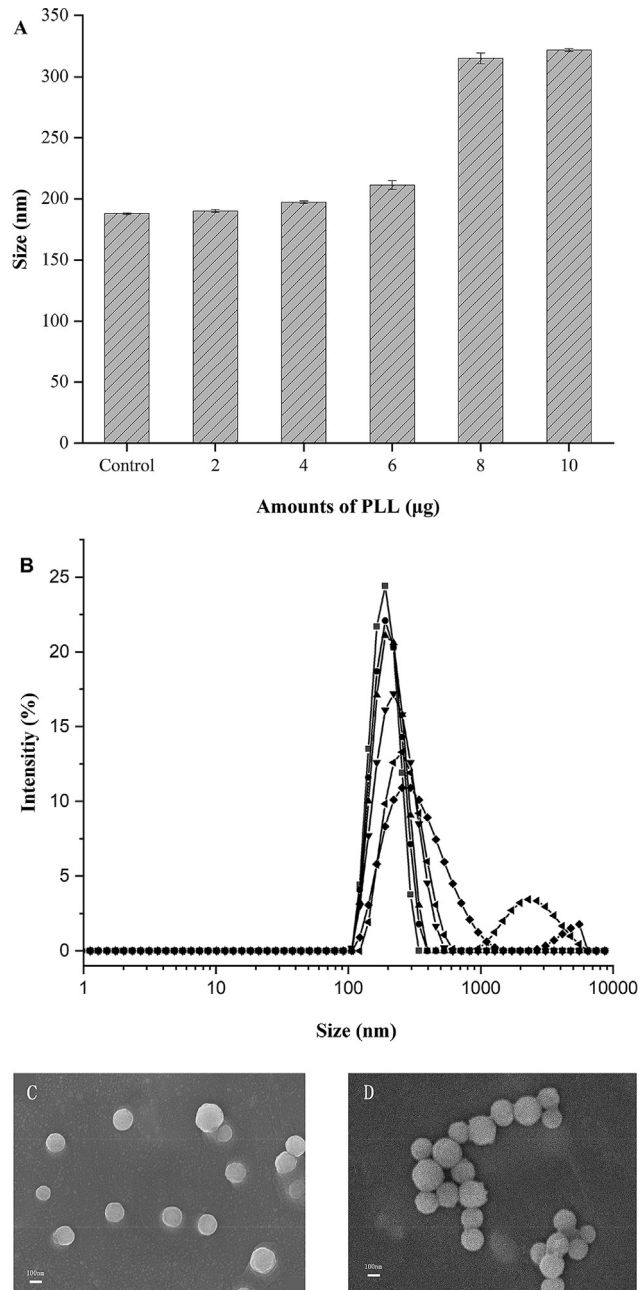


**Fig. 2.** Characterisation of  $\text{Fe}_3\text{O}_4$  NPC: (A) hydrodynamic sizes of  $\text{Fe}_3\text{O}_4$  NPC (Control:  $\text{Fe}_3\text{O}_4$  NP); (B) hydrodynamic size distribution profiles of  $\text{Fe}_3\text{O}_4$  NPC with different amounts of PLL (■, control; ●, 2  $\mu\text{g}$ ; ▲, 4  $\mu\text{g}$ ; ▼, 6  $\mu\text{g}$ ; ◆, 8  $\mu\text{g}$ ; ◀, 10  $\mu\text{g}$ ); (C) SEM images of  $\text{Fe}_3\text{O}_4$  nanoparticles; (D) SEM images of  $\text{Fe}_3\text{O}_4$  NPC.

Therefore, the increment in the hydrodynamic size indicated that streptavidin successfully modified  $\text{Fe}_3\text{O}_4$  NPC via the amidation reaction.

To obtain further evidence that streptavidin was already conjugated with  $\text{Fe}_3\text{O}_4$  NPC, we also measured the change in the zeta potential. The zeta potential of the mother nanoparticles was negative due to the carbonyl moieties of  $\text{Fe}_3\text{O}_4$  nanoparticles. After conjugation with PLL, the zeta potential decreased from  $-30.03$  mV to  $-30.57$  mV did not significantly change ( $P > 0.05$ ). As shown in Fig. 3B, after conjugation with streptavidin, the zeta potential of the  $\text{Fe}_3\text{O}_4$  NPC surface changed from  $-30.57$  mV to  $-25.63$  mV. In comparison with  $\text{Fe}_3\text{O}_4$  NPC, the zeta potential of  $\text{Fe}_3\text{O}_4$  NPC-SA

increased significantly ( $P < 0.05$ ), indicating the successful modification with streptavidin.

### 3.3. Optimisation of experimental parameters

To obtain optimal experiment results, four experimental parameters, namely, concentrations of capture antibody and biotin-antibody, amount of  $\text{Fe}_3\text{O}_4$  NPC-SA, and incubation time between biotin-antibody and  $\text{Fe}_3\text{O}_4$  NPC-SA were optimised using the *Salmonella* concentration at  $8.6 \times 10^7$  cfu  $\text{mL}^{-1}$ . Fig. 4A presents the effect of the concentration of the capture antibody on  $\Delta T_2$ . The  $\Delta T_2$  reached the maximum value at the concentration of

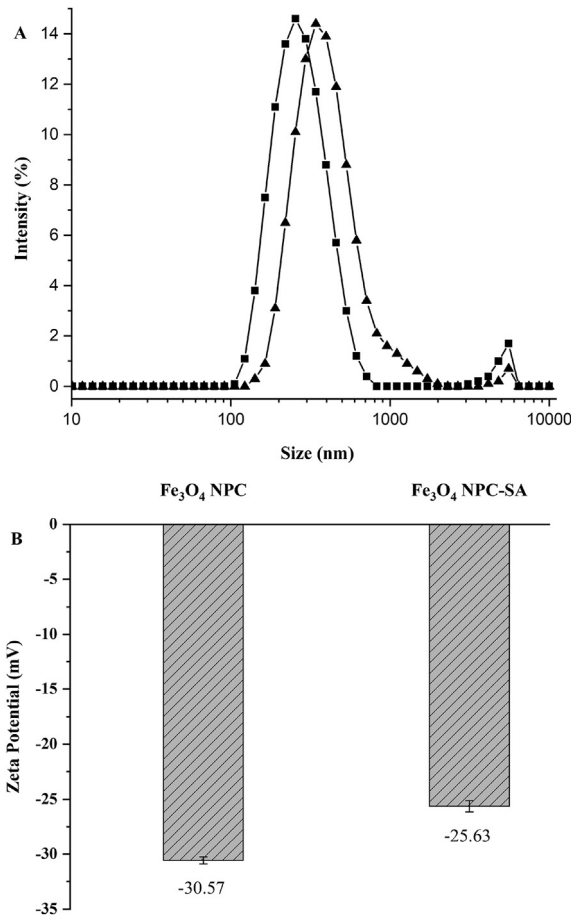


**Fig. 3.** Characterisation of Fe<sub>3</sub>O<sub>4</sub> NPC-SA: (A) hydrodynamic size distribution of Fe<sub>3</sub>O<sub>4</sub> NPC (■) and after the conjugation reaction with streptavidin (▲) and (B) zeta potentials of Fe<sub>3</sub>O<sub>4</sub> NPC and Fe<sub>3</sub>O<sub>4</sub> NPC-SA.

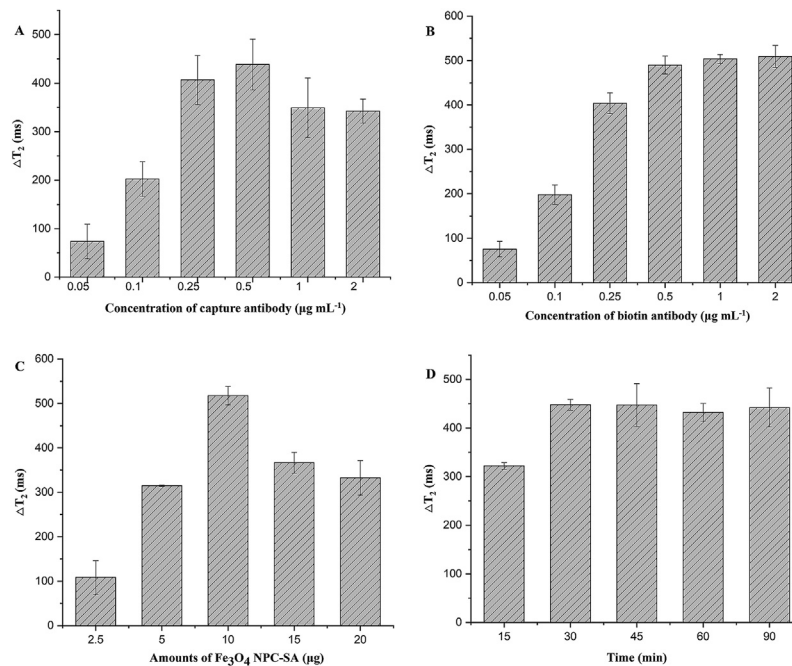


**Fig. 4.** Optimisation of the experimental parameters: (A) concentration of capture antibody; (B) concentration of biotin-antibody; (C) amount of streptavidin-labelled magnetic nanoparticle (Fe<sub>3</sub>O<sub>4</sub> NPC-SA); (D) reaction time between streptavidin conjugated on Fe<sub>3</sub>O<sub>4</sub> NPC and biotin-antibody. The error bars represent the standard deviation of three measurements. All other conditions were the chosen optimal conditions. The error bars represent the average ΔT<sub>2</sub> of triplicate assay.

0.5 μg mL<sup>-1</sup> ( $P < 0.05$ ), and ΔT<sub>2</sub> decreased with further increase in the concentration of the capture antibody. Fig. 4B shows that the ΔT<sub>2</sub> did not significantly change ( $P > 0.05$ ) when the concentration of biotin-antibody was above 0.5 μg mL<sup>-1</sup>. These results indicated that the ΔT<sub>2</sub> reached saturation at a concentration of 0.5 μg mL<sup>-1</sup>. As shown in Fig. 4C, the ΔT<sub>2</sub> reached the maximum value when using 10 μg of Fe<sub>3</sub>O<sub>4</sub> NPC-SA ( $P > 0.05$ ). To save time in the experiment, we studied the incubation period for biotin-antibody and Fe<sub>3</sub>O<sub>4</sub> NPC-SA. As shown in Fig. 4D, the optimal incubation time between biotin-antibody and Fe<sub>3</sub>O<sub>4</sub> NPC-SA was 30 min ( $P < 0.05$ ). Thus, the optimal experimental parameters included the following: 0.5 μg mL<sup>-1</sup> capture antibody were injected into the 96-well microplates and incubated overnight at 4 °C; 0.5 μg mL<sup>-1</sup> biotin-antibody were added to the 96-well microplates and incubated for 1 h at 37 °C; and 10 μg of Fe<sub>3</sub>O<sub>4</sub> NPC-SA were added into the microplates and incubated for 30 min.

### 3.4. Specificity and detection limit of NMR biosensor

To confirm the feasibility of the NMR biosensor, we tested specificity by replacing *Salmonella* with other non-target bacterial strains such as *L. monocytogenes* (ATCC 19115), *P. vulgaris* (CMCC 49027), *P. aeruginosa* (CMCC 11997), and *Shigella sonnei* (Jiangxi CDC isolates) at a concentration of 10<sup>7</sup> cfu mL<sup>-1</sup>. The bacterial solution was replaced by PBS in the negative control. Fig. 5A shows that the ΔT<sub>2</sub> evidently increased in the solution added with the target bacteria compared with those in the solutions with the other interfering bacteria ( $P < 0.05$ ). No significant variation in T<sub>2</sub> was found in the control, indicating that the change in T<sub>2</sub> was attributed to the special recognition among capture antibody, *Salmonella*, biotin-antibody, and Fe<sub>3</sub>O<sub>4</sub> NPC-SA.

The sensitivity of the NMR biosensor for detecting *Salmonella* under the optimised conditions was also determined. As shown in Fig. 5B, the ΔT<sub>2</sub> of the sample varied in *Salmonella* concentrations of 8.6 × 10<sup>1</sup>–8.6 × 10<sup>7</sup> cfu mL<sup>-1</sup>. We identified different ΔT<sub>2</sub> between

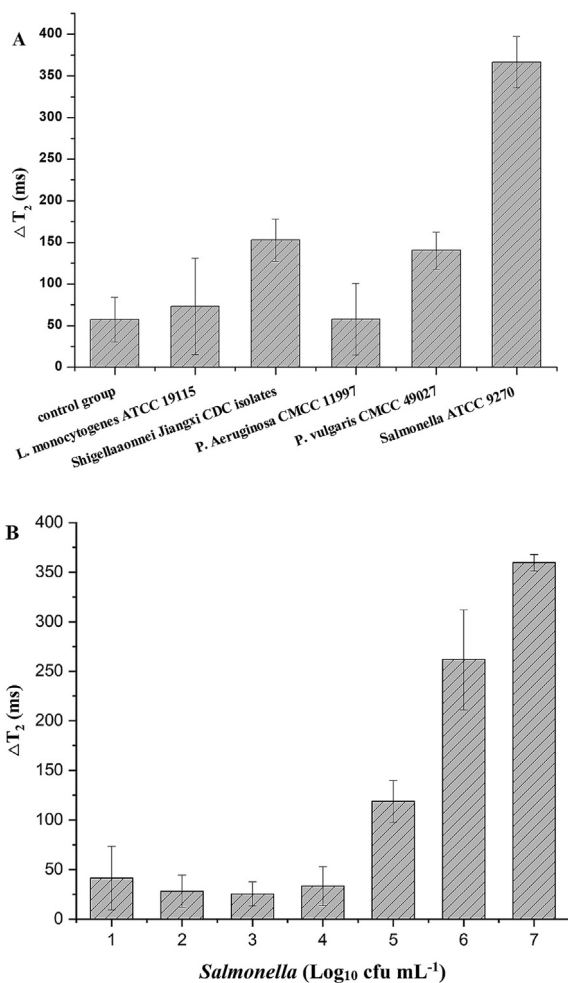


**Fig. 5.** Specificity and detection limit of NMR biosensor: (A) specificity of NMR biosensor for *Salmonella*, *L. monocytogenes*, *P. vulgaris*, *P. aeruginosa*, and *Shigella sonnei* (the concentrations of all bacteria were  $10^7$  cfu  $\text{mL}^{-1}$ ) and (B) sensitivity of NMR biosensor. All experiments were performed under the optimal conditions. The error bars represent the average  $\Delta T_2$  of triplicate assays.

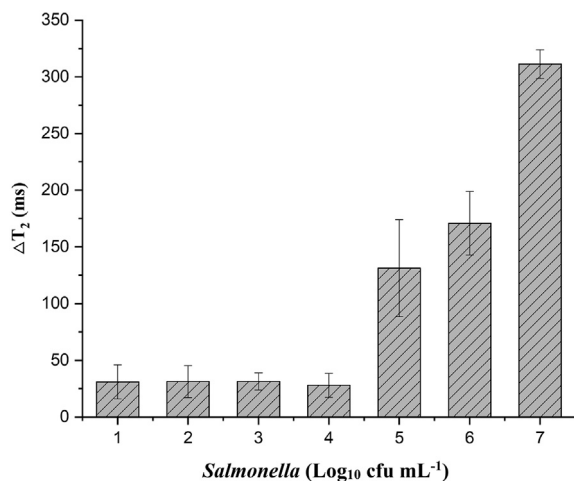


**Fig. 6.** Sensitivity of NMR biosensor in milk samples. All experiments were performed under the optimal conditions. The error bars represent the average  $\Delta T_2$  of triplicate assays.

$10^4$  and  $10^5$  cfu  $\text{mL}^{-1}$  *Salmonella* ( $P < 0.05$ ). Hence, the LOD of the NMR biosensor for *Salmonella* detection was  $10^5$  cfu  $\text{mL}^{-1}$ .

### 3.5. Milk sample analysis

To determine the application of the developed NMR biosensor, we tested it for detection of *Salmonella* in spiked milk samples. As shown in Fig. 6, the  $\Delta T_2$  value was negligible within the concentration range of  $10^1$ – $10^4$  cfu  $\text{mL}^{-1}$  *Salmonella* but increased significantly with increasing *Salmonella* concentration from  $10^5$  cfu  $\text{mL}^{-1}$  to  $10^7$  cfu  $\text{mL}^{-1}$  ( $P < 0.05$ ). These results indicated that the LOD of the NMR biosensor for *Salmonella* detection was  $10^5$  cfu  $\text{mL}^{-1}$  in milk samples.

## 4. Conclusion

In conclusion, a NMR biosensor for rapid detecting *Salmonella* in milk has been successfully developed. In this method, the magnetic particles used as probe would reduce the  $T_2$  of the water protons. To improve the sensitivity of the NMR biosensor, we adopted two signal amplification methods including streptavidin–biotin system and magnetic nanoparticles cluster. As predicted, the sensitivity of the NMR biosensor increased significantly, that is, it can detect *Salmonella* up to  $10^5$  cfu  $\text{mL}^{-1}$ .

In this paper, the strategy of cross-linking interaction model of nanoparticle will provide guidance for design of nanoparticle NMR signal amplification biosensors. Compared with convenient approaches, pre-treatments, such as nucleic acid extraction, are not required, thereby allowing rapid and simple assay of pathogens. The proposed would take 160 min to complete all the tests given that a ready-to-use microplate has already been prepared. The method is faster than classical culture methods. Evidently, the proposed method is a rapid, simple, and novel technology for detecting foodborne bacteria in food matrices. Moreover, the established detection system can be widely used for detection in other fields including medical, environmental, and agricultural sectors.

## Acknowledgements

This work was supported by the National Natural Science Foundation of China (Beijing; 31860467) and the Science and Technology Planning Project of Jiangxi Province (Nanchang, China; 20151BBG70049).

## References

- Alcantara, D., Lopez, S., Garcia-Martin, M., & Pozo, D. (2016). Iron oxide nanoparticles as magnetic relaxation switching (MRSw) sensors: Current applications in nanomedicine. *Nanomedicine*, 12, 1253–1262.
- Bai, J., Trinetta, V., Shi, X., Noll, L. W., Magossi, G., Zheng, W., et al. (2018). A multiplex real-time PCR assay, based on *invA* and *pagC* genes, for the detection and quantification of *Salmonella enterica* from cattle lymph nodes. *Journal of Microbiological Methods*, 148, 110–116.
- Cai, S., Liang, G., Zhang, P., Chen, H., Zhang, S., Liu, B., et al. (2011a). Rational strategy of magnetic relaxation switches for glycoprotein sensing. *Analyst*, 136, 201–204.
- Cai, S., Liang, G., Zhang, P., Chen, H., Zhang, S., Liu, B., et al. (2011b). A miniature chip for protein detection based on magnetic relaxation switches. *Biosensors and Bioelectronics*, 26, 2258–2263.
- Chen, Y., Zou, M., Wang, D., Li, Y., Xue, Q., Xie, M., et al. (2013). An immunosensor based on magnetic relaxation switch and polystyrene microparticle-induced immune multivalency enrichment system for the detection of *Pantoea stewartii* subsp. *Stewartii*. *Biosensors and Bioelectronics*, 43, 6–11.
- Claeys, W. L., Verraes, C., Cardoen, S., De Block, J., Huyghebaert, A., Raes, K., et al. (2014). Consumption of raw or heated milk from different species: An evaluation of the nutritional and potential health benefits. *Food Control*, 42, 188–201.

- Colombo, M., Ronchi, S., Monti, D., Corsi, F., Trabucchi, E., & Prosperi, D. (2009). Femtomolar detection of autoantibodies by magnetic relaxation nanosensors. *Analytical Biochemistry*, 392, 96–102.
- Costard, S., Espejo, L., Groenendaal, H., & Zagmutt, F. J. (2017). Outbreak-related disease burden associated with consumption of unpasteurized cow's milk and cheese, United States, 2009–2014. Centers for Disease Control and Prevention *Emerging Infectious Diseases*, 23. Article 15-1603-t1.
- D'Amico, D. J., & Donnelly, C. W. (2009). Detection, isolation, and incidence of *Listeria* spp. in small-scale artisan cheese processing facilities. A methods comparison. *Journal of Food Protection*, 72, 2499–2507.
- Galikowska, E., Kunikowska, D., Tokarska-Pietrzak, E., Dziadziszko, H., Los, J. M., Golec, P., et al. (2011). Specific detection of *Salmonella enterica* and *Escherichia coli* strains by using ELISA with bacteriophages as recognition agents. *European Journal of Clinical Microbiology & Infectious Diseases*, 30, 1067–1073.
- Grimm, J., Perez, J. M., Josephson, L., & Weissleder, R. (2004). Novel nanosensors for rapid analysis of telomerase activity. *Cancer Research*, 64, 639–643.
- Gruskiene, R., Krivorotova, T., Staneviciene, R., Ratautas, D., Serviene, E., & Sereikaite, J. (2018). Preparation and characterization of iron oxide magnetic nanoparticles functionalized by nisin. *Colloids and Surfaces B: Biointerfaces*, 169, 126–134.
- Haun, J. B., Yoon, T. J., Lee, H., & Weissleder, R. (2010). Magnetic nanoparticle biosensors. *WIREs Nanomedicine and Nanobiotechnology*, 2, 291–304.
- Jain, S., Chattopadhyay, S., Jackeray, R., Abid, C. K., Kohli, G. S., & Singh, H. (2012). Highly sensitive detection of *Salmonella typhi* using surface aminated polycarbonate membrane enhanced-ELISA. *Biosensors and Bioelectronics*, 31, 37–43.
- Jans, H., Liu, X., Austin, L., Maes, G., & Huo, Q. (2009). Dynamic light scattering as a powerful tool for gold nanoparticle bioconjugation and biomolecular binding studies. *Analytical Chemistry*, 81, 9425–9432.
- Kant, K., Shahbazi, M. A., Dave, V. P., Ngo, T. A., Chidambara, V. A., Than, L. Q., et al. (2018). Microfluidic devices for sample preparation and rapid detection of foodborne pathogens. *Biotechnology Advances*, 36, 1003–1024.
- Kim, G. Y., Josephson, L., Langer, R., & Cima, M. J. (2007). Magnetic relaxation switch detection of human chorionic gonadotropin. *Bioconjugate Chemistry*, 18, 2024–2028.
- Law, J. W. F., Ab Mutalib, N. S., Chan, K. G., & Lee, L.-H. (2015). Rapid methods for the detection of foodborne bacterial pathogens: Principles, applications, advantages and limitations. *Frontiers in Microbiology*, 5. Article 770.
- Liu, C., Jia, Q., Yang, C., Qiao, R., Jing, L., Wang, L., et al. (2011). Lateral flow immunochromatographic assay for sensitive pesticide detection by using Fe<sub>3</sub>O<sub>4</sub> nanoparticle aggregates as color reagents. *Analytical Chemistry*, 83, 6778–6784.
- Ma, W., Chen, W., Qiao, R., Liu, C., Yang, C., Li, Z., et al. (2009). Rapid and sensitive detection of microcystin by immunosensor based on nuclear magnetic resonance. *Biosensors and Bioelectronics*, 25, 240–243.
- Matthew, O. D. (2018). Magnetic nanoparticles as contrast agents for molecular imaging in medicine. *Physica C: Superconductivity*, 548, 103–106.
- Mazumdar, S. D., Barlen, B., Kampfer, P., & Keusgen, M. (2010). Surface plasmon resonance (SPR) as a rapid tool for serotyping of *Salmonella*. *Biosensors and Bioelectronics*, 25, 967–971.
- Meng, X., Li, F., Li, F., Xiong, Y., & Xu, H. (2017). Vancomycin modified PEGylated-magnetic nanoparticles combined with PCR for efficient enrichment and detection of *Listeria monocytogenes*. *Sensors and Actuators B: Chemical*, 247, 546–555.
- Perez, J., Simeone, F., Saeki, Y., Josephson, L., & Weissleder, R. (2003). Viral-induced self-assembly of magnetic nanoparticles allows the detection of viral particles in biological media. *Journal of the American Chemical Society*, 125, 10192–10193.
- Shen, J., Zhang, Y., Yang, H., Yang, Y., Zhou, Z., & Yang, S. (2014). Detection of melamine by a magnetic relaxation switch assay with functionalized Fe/Fe<sub>3</sub>O<sub>4</sub> nanoparticles. *Sensors and Actuators B: Chemical*, 203, 477–482.
- Son, J. R., Kim, G., Kothapalli, A., Morgan, M. T., & Ess, D. (2007). Detection of *Salmonella enteritidis* using a miniature optical surface plasmon resonance biosensor. *Journal of Physics: Conference Series*, 61, 1086–1090.
- Taylor, A. D., Ladd, J., Yu, Q., Chen, S., Homola, J., & Jiang, S. (2006). Quantitative and simultaneous detection of four foodborne bacterial pathogens with a multi-channel SPR sensor. *Biosensors and Bioelectronics*, 22, 752–758.
- Wang, J., Li, R., Hu, L., Sun, X., Wang, J., & Li, J. (2016). Development of a quantitative fluorescence single primer isothermal amplification-based method for the detection of *Salmonella*. *International Journal of Food Microbiology*, 219, 22–27.
- Wang, S., Zhang, Y., An, W., Wei, Y., Liu, N., Chen, Y., et al. (2015). Magnetic relaxation switch immunosensor for the rapid detection of the foodborne pathogen *Salmonella enterica* in milk samples. *Food Control*, 55, 43–48.
- Yang, H., Tian, Z., Wang, J., & Yang, S. (2012). A magnetic resonance imaging nanosensor for Hg (II) based on thymidine-functionalized supermagnetic iron oxide nanoparticles. *Sensors and Actuators B: Chemical*, 161, 429–433.
- Yang, Y., Zhang, Y., Shen, J.-C., Yang, H., Zhou, Z.-G., & Yang, S.-P. (2016). A highly selective magnetic sensor with functionalized Fe/Fe<sub>3</sub>O<sub>4</sub> nanoparticles for detection of Pb<sup>2+</sup>. *Chinese Chemical Letters*, 27, 891–895.
- Zhang, L., Huang, R., Liu, W., Liu, H., Zhou, X., & Xing, D. (2016). Rapid and visual detection of *Listeria monocytogenes* based on nanoparticle cluster catalyzed signal amplification. *Biosensors and Bioelectronics*, 86, 1–7.
- Zhang, Y., Zhao, Y., Yang, Y., Shen, J., Yang, H., Zhou, Z., et al. (2015). A bifunctional sensor based on Au-Fe<sub>3</sub>O<sub>4</sub> nanoparticle for the detection of Cd<sup>2+</sup>. *Sensors and Actuators B: Chemical*, 220, 622–626.
- Zhao, Y., Li, Y., Jiang, K., Wang, J., White, W. L., Yang, S., et al. (2017). Rapid detection of *Listeria monocytogenes* in food by biofunctionalized magnetic nanoparticle based on nuclear magnetic resonance. *Food Control*, 71, 110–116.
- Zheng, J., Nie, Y., Hu, Y., Li, J., Li, Y., Jiang, Y., et al. (2013). Time-resolved fluorescent detection of Hg<sup>2+</sup> in a complex environment by conjugating magnetic nanoparticles with a triple-helix molecular switch. *Chemical Communications*, 49, 6915–6917.
- Zhou, B., Liang, T., Zhan, Z., Liu, R., Li, F., & Xu, H. (2017). Rapid and simultaneous quantification of viable *Escherichia coli* O157:H7 and *Salmonella* spp. in milk through multiplex real-time PCR. *Journal of Dairy Science*, 100, 8804–8813.